Available online at www.sciencedirect.com

ScienceDirect

Nuclear and Particle Physics Proceedings 273–275 (2016) 2226–2231

www.elsevier.com/locate/nppp

Measurement of the charged triple gauge boson couplings at the ILC

Aura Rosca

DESY, Notkestr. 85, 22607 Hamburg, Germany

Abstract

After the discovery of the Higgs boson it became even more important to perform precision measurements and to search for deviations from the Standard Model predictions in the electroweak sector. A study of the measurement of trilinear gauge couplings is presented looking at the W-pair production where one W decays leptonically and the other hadronically in e^+e^- annihilation at the ILC at a centre-of-mass energy of 1 TeV with polarized beams. The analysis is based on a realistic full simulation of this process in the ILD detector. We employed a maximum likelihood analysis of a three-dimensional differential cross section based on the angular distributions of the Ws and their decay products. A high sensitivity in the range of 10^{-4} can be obtained at the ILC at $\sqrt{s} = 1$ TeV.

Keywords: electron positron colliding beams, beam polarization, W pair production, W leptonic decay, W hadronic decay, coupling 3 gauge bosons

1. Introduction

The non-Abelian structure of the gauge group describing the fundamental interactions implies that the electroweak gauge bosons γ, W and Z interact among themselves and give rise to charged triple (and quartic) vertices of the type $WW\gamma$ and WWZ. The Standard Model (SM) makes precise predictions for the form of these gauge boson self-couplings. Their measurement represents a fundamental test of the gauge structure of the SM and at the same time any possible deviation from expectations would be a clear indication of new physics at higher energy scale.

Assuming only Lorentz invariance, the most general form of a trilinear gauge-boson vertex (TGV), WWZ or $WW\gamma$, is described by seven complex parameters [1]. Regarding only the CP-conserving couplings and assuming electromagnetic gauge invariance, six trilinear gauge-boson couplings (TGCs) remain. These are g_1^Z, g_5^Z, κ_γ, λ_γ, κ_Z and λ_Z. Within the SM, $g_1^Z = \kappa_\gamma = \kappa_Z = 1$ and $g_5^Z = \lambda_\gamma = \lambda_Z = 0$ at tree level. With the exception of g_5^Z these TGCs also conserve C and P separately. The requirement of local SU(2) gauge invariance leads to additional constraints and reduces the number of couplings to three parameters.

We performed a study of the TGCs g_1^Z, κ_γ and λ_γ assuming the constraints above, however beam polarization at the ILC will allow us to access the full set of couplings.

At lepton colliders TGVs can be studied through processes such as W-pair production, single-W production and single-photon production.

To lowest order within the SM, three Feynman diagrams contribute to W-pair production: the t-channel neutrino exchange and the s-channel γ and Z exchanges. The s-channel diagrams contain both WWZ and $WW\gamma$ vertices, such giving access to the relevant couplings. The $WW\gamma$ vertex also appears in one of the t-channel diagrams that contribute to the single-W production and to the single-γ production through W-boson fusion.

In this article we report about the achievable precision on the measurement of the TGCs of the W boson at the future International Linear Collider operated at $\sqrt{s} = 1$ TeV. The results are based on analyses of multi-differential cross section in W-pair production. Previous results on TGCs at the ILC were published in ref. [2].

Currently the best direct measurements of the TGC

http://dx.doi.org/10.1016/j.nuclphysbps.2015.09.362

couplings come from the experiments at LEP and the LHC [3]. The errors on these measurements are of the order of a few percent.

2. Physics simulation at the ILC

Signal and background events are generated using the WHIZARD [4] event generator. The effects of initial state radiation and beamstrahlung are included. The four-momenta of the final-state quarks and leptons are passed as input to PYTHIA 6.422 [5] for parton showering and hadronization. The detector response is simulated using the MOKKA [6] full Monte Carlo detector simulation.

Events were generated at a centre-of-mass energy of 1 TeV assuming 100% polarized beams. To obtain different polarization configurations events were properly mixed. The final results are reported for an integrated luminosity of $\mathcal{L} = 1000\ fb^{-1}$.

The cross section for $\gamma\gamma \rightarrow$ hadrons events, with mass exceeding 2 GeV, is several hundred nb [7]. This means about 4.1 events of this type are produced per bunch crossing. These events (pile-up) are overlaid to the physics events. Since the pile-up events are produced in the t-channel q-exchange most of the resulting final state particles are distributed at low angles.

2.1. Event selection

W bosons decay into hadrons, mostly through $W \rightarrow ud$ or cs, or leptons, $W^- \rightarrow \ell^-\nu$, where ℓ denotes an electron, muon or tau lepton. W-boson pair production yields three classes of events: the fully-leptonic, $\ell\nu\ell\nu$, the semi-leptonic, $qq\ell\nu$, and the fully-hadronic, $qqqq$, final states. Due to the presence of more than one neutrino in the $\ell\nu\ell\nu$ final state, the masses of the W bosons cannot be directly reconstructed from their decay products. This is why this decay channel is not further considered. The $qqqq$ final state has been excluded as well due to the fact that the charge of the W-boson cannot be reconstructed with sufficient precision from the jets of the hadronic decay.

We only considered here the mixed hadronic/leptonic topology from the decay of a W-pair event. This topology has good statistics and can be separated from the background with a high degree of purity allowing us to reconstruct all final state variables. A considerable advantage of the mentioned topology is that it allows the determination of the charge of the W from the charge of the lepton.

Visible final-state fermions are reconstructed in each event. Electrons and muons from W-boson decays are measured in the calorimeters and in the tracking system. Lepton candidates are defined by the following ratios: E_{ECAL}/E_{tot} and E_{tot}/p_{track}, where E_{ECAL} is the energy measured in the electromagnetic calorimeter, E_{tot} is the total measured energy in the calorimeters, and p_{track} is the measured track momentum in the tracking detectors. We require that E_{ECAL}/E_{tot} be greater than 0.9 for electrons and less than 0.5 for muons and E_{tot}/p_{track} be greater than 0.8 for electrons and below 0.4 for muons. Jets that originate from quarks are reconstructed by combining information from calorimetric clusters and associated tracks and using the k_T algorithm [8], see subsection 2.2.

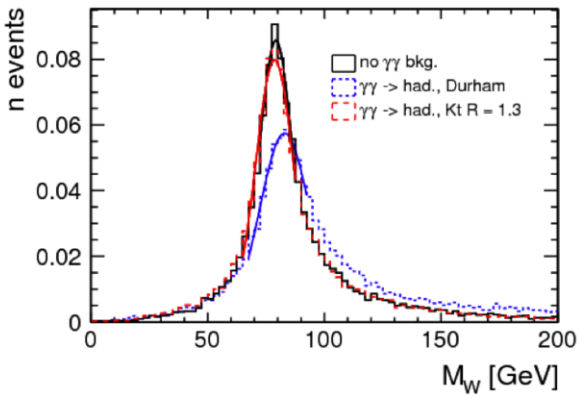

Figure 1: Distributions of the reconstructed invariant mass of the W-boson using different jet clustering algorithms. The black curve is obtained for events without $\gamma\gamma$ overlay.

The event selection is a simple cut-based selection aiming to identify an isolated lepton. This is set aside and the rest of the event is clustered in two jets. We impose kinematic constraints including energy and momentum conservation and equal mass constraint for the reconstructed W bosons.

2.2. Jet clustering and suppression of $\gamma\gamma$ overlay events

We employ a jet-clustering algorithm to separate the event into 2 jets, after taking out the isolated lepton.

At the ILC, the physics event is accompanied by significant additional energy from $\gamma\gamma \rightarrow$ hadrons background. For this reason it is not possible to use the jet clustering algorithms developed for LEP which combine all particles into jets. We found that the k_T algorithms [8] developed for hadron collisions are more suitable since they reduce the inclusion of background particles into jets from the e^+e^- interaction. We compared the reconstructed visible energy observed with the

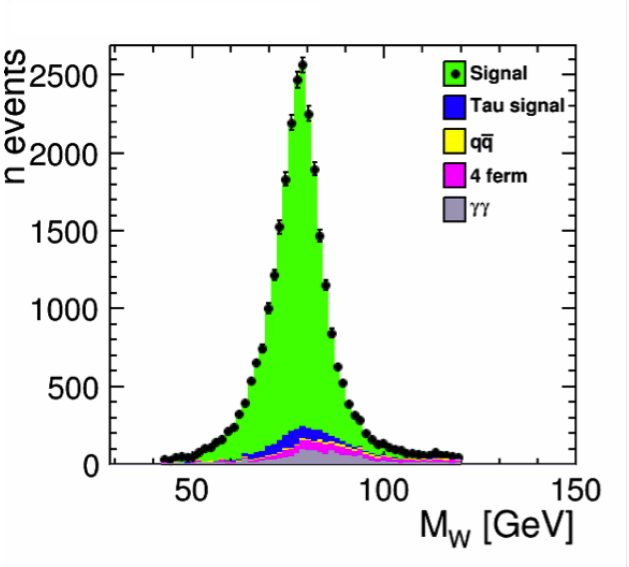

Figure 2: Distribution of the reconstructed W-boson mass after applying the kinematic fit using the equal-mass constraint and all selection cuts.

Durham algorithm to that obtained with the k_T algorithm for different values of the jet radius parameter R. The Durham algorithm adds about 100 GeV of energy from the background to the reconstructed jets, while this effect is reduced using the k_T algorithm. As an example, the reconstruction of the W bosons is illustrated in figure 1. The distributions obtained with and without the overlay of $\gamma\gamma$ events are compared.

Jets are reconstructed from particle flow objects using the k_T algorithm in its exclusive mode with R = 1.3 and using the E recombination scheme. The clustering algorithm ends when two jets are found.

2.3. Kinematic fit

A kinematic fit, assuming four-momentum conservation and other constraints, is used to improve energy and angular resolutions. The four-momentum conservation requirement determines for our final state the momentum and the direction of the neutrino. The mass resolution of the two W bosons is improved by the additional constraint of requiring their masses to be equal. This procedure results in a two-constraint fit (2C) of $qq\ell\nu$ events. The kinematic fit also takes into account the effect of the ISR photons, as in reference [9].

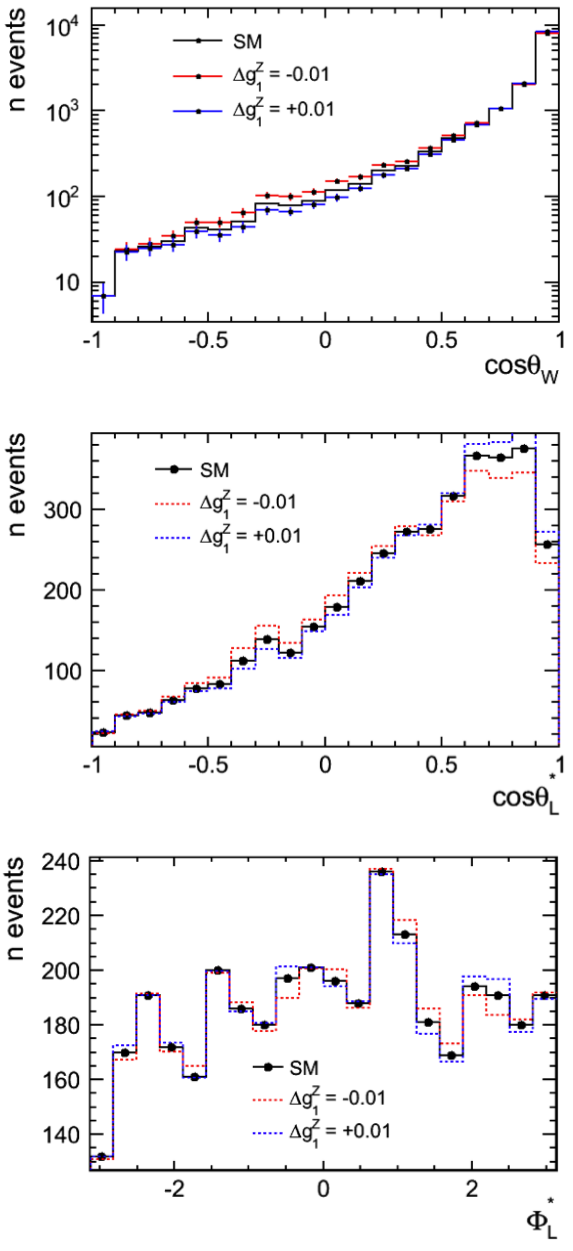

Figure 3: Distributions of the reconstructed polar scattering angle, a) $\cos\theta_W$, of the W^- boson in $qq\ell\nu$ W-pair events and of the reconstructed W decay angles, b) $\cos\theta_L$ and c) ϕ_L. The data at $\sqrt{s} = 1$ TeV are shown, together with the expectations for the SM ($\Delta g_1^Z = 0$) and for anomalous TGCs, (Δg_1^Z = -0.01 and Δg_1^Z = +0.01). Distributions of the W decay angles are shown here for values of $\cos\theta_W < 0.8$.

The suppression of the $qq\tau\nu$ events is performed using the same discriminating variable τ_{disc} as defined in reference [10]. Candidates with $\tau_{disc} < 1$ are considered $qq\tau\nu$ events and rejected.

The total signal efficiency is estimated to be 16% in

the presence of pile-up events. The purity of the selection is 87% at 1 TeV. The residual background not originating from W-boson pair production is dominated by $\gamma\gamma$ events (38%), followed by $qqe\nu$ events (28%). The $qq\tau\nu$ events amount to 23%. The $qqe\nu$ events considered here as a background originate either from single-W production or fail the signal definition:

$$M_W - 50\ \text{GeV} < M_{qq/\ell\nu} < M_W + 50\ \text{GeV}.$$

The distribution of M_W after applying all the cuts is shown in figure 2.

3. Extraction of TGCs for W^+W^- events

In the W-pair production process, all information about production and decay is contained in five variables: the production angle θ_W of the W^- and the polar and azimuthal angles θ_L, ϕ_L and θ_H, ϕ_H of the decay products in the rest frame of the decaying W^- and W^+ relative to the W flight direction. In our study, the differential distribution in the W^- polar angle, θ_W, and the two decay angles of the leptonically decaying W-boson, θ_L and ϕ_L, are used for the determination of the TGCs. The corresponding three distributions are shown in figure 3 for the SM predictions and for the expectations of two anomalous values of the coupling Δg_1^Z, where Δ stands for the difference from the SM value. Fits to all three TGCs Δg_1^Z, $\Delta\kappa_\gamma$ and $\Delta\lambda_\gamma$ are performed.

Monte Carlo signal events were reweighted to correspond to different values of the gauge couplings and the reweighted distributions were compared to those representing the data, as in reference [10]. Weights were obtained using the matrix element calculations from WHIZARD.

To each event the weight is applied:

$$\begin{aligned} R(\Delta g_1^Z, \Delta\kappa_\gamma, \Delta\lambda_\gamma) = 1 &+ A\Delta g_1^Z + B\Delta\kappa_\gamma + C\Delta\lambda_\gamma \\ &+ D\Delta g_1^{Z^2} + E\Delta\kappa_\gamma^2 + F\Delta\lambda_\gamma^2 + G\Delta g_1^Z\Delta\kappa_\gamma + H\Delta g_1^Z\Delta\lambda_\gamma \\ &+ I\Delta\lambda_\gamma\Delta\kappa_\gamma, \end{aligned}$$

where Δg_1^Z, $\Delta\kappa_\gamma$ and $\Delta\lambda_\gamma$ are free parameters. The function $R(\Delta g_1^Z, \Delta\kappa_\gamma, \Delta\lambda_\gamma)$ describes the quadratic dependence of the cross-section on the coupling parameters. SM events with $\Delta g_1^Z = \Delta\kappa_\gamma = \Delta\lambda_\gamma = 0$ are used to recalculate the matrix elements of the events for a set of nine different combinations of Δg_1^Z, $\Delta\kappa_\gamma$ and $\Delta\lambda_\gamma$ values, as shown in table 1. The resulting weight is given by the ratio of the new matrix element values compared to the SM ones, the R_i. The event kinematics is unchanged.

Using table 1, we get for the R_i ratios:

$$\begin{aligned}
R_1 &= 1 + A\left|\Delta g_1^Z\right| + D\left|\Delta g_1^Z\right|^2, \\
R_2 &= 1 + B\left|\Delta\kappa_\gamma\right| + E\left|\Delta\kappa_\gamma\right|^2, \\
R_3 &= 1 + C\left|\Delta\lambda_\gamma\right| + F\left|\Delta\lambda_\gamma\right|^2, \\
R_4 &= 1 - A\left|\Delta g_1^Z\right| + D\left|\Delta g_1^Z\right|^2, \\
R_5 &= 1 - B\left|\Delta\kappa_\gamma\right| + E\left|\Delta\kappa_\gamma\right|^2, \\
R_6 &= 1 - C\left|\Delta\lambda_\gamma\right| + F\left|\Delta\lambda_\gamma\right|^{2,}, \\
R_7 &= 1 + A\left|\Delta g_1^Z\right| + B\left|\Delta\kappa_\gamma\right| + D\left|\Delta g_1^Z\right|^2 + E\left|\Delta\kappa_\gamma\right|^2 \\
&\quad + G\left|\Delta g_1^Z\right|\left|\Delta\kappa_\gamma\right|, \\
R_8 &= 1 + B\left|\Delta\kappa_\gamma\right| + C\left|\Delta\lambda_\gamma\right| + E\left|\Delta\kappa_\gamma\right|^2 + F\left|\Delta\lambda_\gamma\right|^2 \\
&\quad + I\left|\Delta\kappa_\gamma\right|\left|\Delta\lambda_\gamma\right|, \\
R_9 &= 1 + A\left|\Delta g_1^Z\right| + C\left|\Delta\lambda_\gamma\right| + D\left|\Delta g_1^Z\right|^2 + F\left|\Delta\lambda_\gamma\right|^2 \\
&\quad + H\left|\Delta g_1^Z\right|\left|\Delta\lambda_\gamma\right|,
\end{aligned}$$

where $\left|\Delta g_1^Z\right| = \left|\Delta\kappa_\gamma\right| = \left|\lambda_\gamma\right| = 0.001$. The coefficients A, B, C, D, E, F, G, H and I are deduced for each event from the nine equations above.

Three-dimensional $(\cos\theta_W, \cos\theta_L, \phi_L)$ event distributions are fitted with MINUIT [11], maximizing a log-likelihood function of Δg_1^Z, $\Delta\kappa_\gamma$ and $\Delta\lambda_\gamma$ and taking the SM Monte Carlo sample as data. The $\cos\theta_W$ distribution is most sensitive, but there is statistically independent information in the other observables that is important when fitting several couplings in the same time.

The log-likelihood function is defined as:

$$\mathcal{L} = \sum_{++,--,+-,-+} \sum_{bins} \left(N_i^{DATA} \log N_i^{MC}(\Delta g_1^Z, \Delta\kappa_\gamma, \Delta\lambda_\gamma) - N_i^{MC}(\Delta g_1^Z, \Delta\kappa_\gamma, \Delta\lambda_\gamma) \right),$$

where N_i^{MC} is the content of the i-th bin of the Monte Carlo distribution weighted as a function of TGCs, and N_i^{DATA} is the content of the corresponding bin for the data. The sum $\sum_{++,--,+-,-+}$ accounts for the different helicity sets used for the measurement. The optimum binning chosen is 10 bins for the $\cos\theta_W$ distribution and 5 bins for each decay angle distribution.

4. Results

The precision achievable on the couplings is shown in table 2. For an integrated luminosity of 1000 fb^{-1}

	R_1	R_2	R_3	R_4	R_5	R_6	R_7	R_8	R_9
Δg_1^Z	+0.001	0	0	-0.001	0	0	+0.001	0	+0.001
$\Delta\kappa_\gamma$	0	+0.001	0	0	-0.001	0	+0.001	+0.001	0
$\Delta\lambda_\gamma$	0	0	+0.001	0	0	-0.001	0	+0.001	+0.001

Table 1: Δg_1^Z, $\Delta\kappa_\gamma$ and $\Delta\lambda_\gamma$ values used to calculate the coefficients.

$\mathcal{P}_{-80,-20} : \mathcal{P}_{-80,+20} : \mathcal{P}_{+80,-20} : \mathcal{P}_{+80,+20}$	Δg_1^Z	$\Delta\kappa_\gamma$	$\Delta\lambda_\gamma$	$\Delta\mathcal{P}_{e^-}$	$\Delta\mathcal{P}_{e^+}$
1:1:1:1	1.88	1.73	2.66	0.0009	0.0014
1:4:4:1	1.92	1.68	2.79	0.0010	0.0017
0:1:1:0	1.89	1.69	2.85	0.0015	0.0023
1:4:4:1 and $\lvert\mathcal{P}_e\rvert \neq -\lvert\mathcal{P}_e\rvert$	1.92	1.68	2.79	0.0016	0.0018

Table 2: Summary of achievable errors ($\times 10^{-4}$) on the gauge couplings and on the two beam polarizations for different running scenarios, using $qq\ell\nu$ events and an integrated luminosity of 1000 fb^{-1} at $\sqrt{s}$ = 1 TeV.

the precision ranges between 2 to 3 $\times$ 10^{-4} for all three couplings. For $\sqrt{s}$ = 1 TeV the correlations in the multi-parameter fits are relativelly small. For instance, the correlation between Δg_1^Z and $\Delta\kappa_\gamma$ is almost 48% while the correlation between $\Delta\lambda_\gamma$ and the other two is about 10%.

Knowledge of the exact polarization is very important due to the fact that deviations from expectations can fake contributions from anomalous couplings. One way to overcome this is to perform a simultaneous measurement of the polarization and gauge couplings.

4.1. Polarization from simultaneous fit

A method to extract the polarization from annihilation data has been proposed by Klaus Mönig in reference [12] and investigated in detailed at $\sqrt{s}$ = 1 TeV in [13]. An additional weight that expresses the dependence on the polarization is applied to the event. The method requires some integrated luminosity with all 4 helicity combinations, optimally equally split between configurations, and the assumption that the absolute value of the polarization stays constant. We have assessed the achievable errors on the polarization when reducing the integrated luminosity spent on the ++ and −− polarization sets. Such configurations of the helicities are of low interest for most of the physics studies, since they suppress the s-channel production. A scenario with only 20% like-sign configuration is close to the optimum and has negligible impact on the TGCs.

Table 2 shows the obtainable errors on the two beam polarizations for two running scenarios: the total integrated luminosity is divided equally between $\mathcal{P}_{-80,+20}$ and $\mathcal{P}_{+80,-20}$ or it is divided among $\mathcal{P}_{-80,-20}, \mathcal{P}_{-80,+20}, \mathcal{P}_{+80,-20}$ and $\mathcal{P}_{+80,+20}$ in the proportions 1:4:4:1. For the latter case, the precision obtained on the electron and positron polarizations is $\Delta\mathcal{P}_{e^-}$ = 0.0010 and $\Delta\mathcal{P}_{e^+}$ = 0.0017, respectively.

We also studied the impact on our results when the absolute values of the left- and right-handed states are not the same and possible corrections have to be obtained from polarimeters with a relative precision of 0.25%. The measured electron polarization is degraded, however the effect on the couplings is negligible.

Assuming an integrated luminosity of 1000 fb^{-1} at $\sqrt{s}$ = 1 TeV, table 2 summarizes the achievable errors on the TGCs and the beam polarizations.

As mentioned in section 3, the method used for the determination of the TGCs profits from including the additional information contained in the distribution of the two decay angles of the hadronically decaying W-boson, θ_H and ϕ_H. Preliminary results on the expected errors for Δg_1^Z, $\Delta\kappa_\gamma$ and λ_γ for $\sqrt{s}$ = 1 TeV with 1000 fb^{-1} are of the order of 0.7 $\times$ 10^{-4}. We have not checked neither the impact on the errors when removing the gauge invariance constraints, nor included in the fit the other gauge couplings. This would be the subject of further analysis.

5. Summary

A future high-energy electron positron linear collider will provide an excellent opportunity for the measurement of the gauge couplings of the W bosons. The achievable precision reaches a few 10^{-4} at $\sqrt{s}$ = 1 TeV.

Such accuracies on the couplings were obtained from a fit with three free parameters of the multi-dimensional angular differential cross section in W-pair production and by restricting the measurement to the three C and P conserving couplings, g_1^Z, κ_γ and λ_γ, and applying gauge invariance.

We currently develop analyses that include more observables and relaxed constrains with the ultimate goal to access the complete set of couplings.

Acknowledgments

I would like to thank my colleagues Klaus Mönig and Ivan Marchesini for their support and many fruitful discussions. I am grateful to the ILC Generators group and the ILD MC production team for providing the data samples used for this study. I would like to acknowledge the support of the DFG through the SFB 676 ”Particles, Strings and the Early Universe”.

References

[1] K. Hagiwara, K.Hikasa, R. D. Pecci, D. Zeppenfeld, Nucl. Phys. B282 (1987) 253; K. Gämers, G. Gounaris, Z. Phys. C1 (1979) 259.
[2] W. Menges, LC-PHSM-2001-022 (2001); P. Bechtle, W. Ehrenfeld, I. Marchesini, LC-DET-2009-003 (2009).
[3] (LEP Collaborations), Phys. Rept. 532 (2013) 119; (ATLAS Collaboration) Phys. Rev. D87 112001 (2013); (CMS Collaboration) Phys. Rev. D89 092005 (2014).
[4] W. Killian, T. Ohl, J. Reuter, Eur. Phys. J. C71 (2011) 1742; arXiv:0708.4233 [hep-ph].
[5] T. Sjoestrand, S. Mrenna, P. Skands, J. High Energy Phys. 05 (2006) 026.
[6] P. Mora de Freitas, H. Videau, LC-TOOL-2003-010 (2003).
[7] The Particle Data Group, K. Hagiwara et al., Phys. Rev. D66 (2002) 010001.
[8] M. Cacciari, G.P. Salam, Phys. Lett. B641 (2006) 57.
[9] M. Bechmann, B. List and J. List, Nucl. Instrum. Meth. A624 (2010) 184.
[10] I. Marchesini, DESY-THESIS-2011-044 (2011).
[11] F. James, CERN Program Library Long Writeup D506.
[12] K. Mönig, LC-PHSM-2000-059 (2000).
[13] A. Rosca, LC-REP-2013-009 (2013).